

Research report

Postnatal hypobaric hypoxia in rats impairs water maze learning and the morphology of neurones and macroglia in cortex and hippocampus

Zuzana Šimonová^{a,c}, Katalin Štěrbová^b, Gustav Brožek^b,
Vladimír Komárek^b, Eva Syková^{a,c,*}

^a Department of Neuroscience, Center for Cell Therapy and Tissue Repair, Charles University, Second Medical Faculty, 150 18 Prague 5, Czech Republic

^b Departments of Child Neurology and Physiology, Charles University, Second Medical Faculty, 150 18 Prague 5, Czech Republic

^c Department of Neuroscience, Institute of Experimental Medicine, ASCR, Vídeňská 1083, 142 20 Prague 4, Czech Republic

Received 16 February 1999; received in revised form 22 October 2002; accepted 22 October 2002

The authors dedicate this paper to the memory of Professor Gustav Brožek, M.D., whose death occurred during the preparation of this manuscript.

Abstract

Newborn rats were exposed to intermittent hypobaric hypoxia from birth until the age of 19 days. Spatial memory was tested in a Morris water maze from postnatal day (P) 23 to P32 and from P100 to P109. From P24 to P27 and on days P100 and P101, the escape latencies of hypoxic animals were longer than those of controls. At P24, the number of neuronal bodies increased in cortical layer II of the somatosensory, motor, and auditory areas, and in layer V of the motor area, but the number of neuronal bodies throughout the whole cortical thickness was unchanged. Decreases in the immunostaining density for neurofilaments (anti-NF 160), astrocytes (anti-GFAP), and oligodendrocytes (RIP) were found in the hippocampus, and the typical parallel organisation of neuronal and macroglial processes was lost. Decreases in immunostaining for neurofilaments and oligodendrocytes were also found in the somatosensory cortex and motor cortex. In adult hypoxic rats, at P114–P240, the number of neuronal bodies and the immunostaining density for neurofilaments, astrocytes, and oligodendrocytes in the examined areas were similar to adult controls; however, in the hippocampus we found hypertrophy of fine astrocytic processes and a decreased number of oligodendrocytic processes. We conclude that the neonatal brain damage induced by hypobaric hypoxia impairs spatial memory in infant as well as adult rats. Hypobaric hypoxia delays the maturation of neurones and substantially affects macroglia in the cortex and hippocampus.

© 2002 Elsevier Science B.V. All rights reserved.

Keywords: Astrocytes; Brain; Immunohistochemistry; Neuronal counting; Oligodendrocytes; Spatial memory

1. Introduction

Perinatal hypoxic–ischemic injury in children often has neurological consequences such as cerebral palsy, mental retardation, seizures or minimal brain dysfunction, depending on the character and severity of the insult. Animal models of hypoxic–ischemic brain injury use cardiac arrest, uni- or bilateral carotid artery ligation and/or exposure to high altitude. The result is usually cortical necrosis, selective neuronal loss or leukomalacia, depending on the age of the animal [9,12,13,26,29]. Neuronal loss can obviously

result in brain dysfunction. After cardiac arrest, Sadowski et al. [26] observed neuronal loss in the hippocampal CA1 region and delayed neuronal loss in the CA3 region.

A role for astrocytes and oligodendrocytes in animal behaviour and learning has also been suggested (for review see [11]). The changes in astrocytes and oligodendrocytes after hypoxia are, however, far from clear. Zimmer et al. [38] observed a marked increase in immunoreactivity for the astrocytic marker glial fibrillary acidic protein (GFAP) after 114 days of chronic normobaric hypoxia with decreased oxygen, but not after 59 days of hypoxic exposure. Dell'Anna et al. [5] observed an increase in GFAP staining in the hippocampus 7 days after hypoxia evoked by nitrogen exposure at P2, but not 14 or 21 days after hypoxia. In the rat cortex at P18, 1 day after intermittent hypobaric hypoxia, Brichová

* Corresponding author. Tel.: +420-2-4106-2204; fax: +420-2-4106-2783.

E-mail address: sykova@biomed.cas.cz (E. Syková).

[3] observed only a mild effect on astrocytes, which showed swollen end-feet when examined by electron microscopy, and she did not observe any changes in oligodendrocytes; however, delayed myelination after intermittent hypobaric hypoxia was observed by Langmeier et al. [12].

The Morris water maze [18] is often used for testing spatial memory in the rat. The animals are placed into a circular water tank with a visible or an invisible platform. They can easily find the visible platform, but when searching for the hidden one they have to learn the arrangement of surrounding objects and their spatial relationship to the platform in order to find it. The rats are not able to find the invisible platform after hippocampal damage [6]. Ontogeny studies of spatial navigation were performed by Schenk [28] and Rudy et al. [25]. A visible cue in the water maze can be easily localised by 19-day-old rats, an invisible platform only by rats older than 21 days. Behavioural studies have searched for hyperactivity, altered learning or avoidance behaviour and changes in spontaneous behaviour [15,37]. To our knowledge, there has been no previous study examining how intermittent hypobaric hypoxia affects spatial memory in infant rats.

The significance of glial cells for the maintenance of accurate synaptic transmission and the homeostasis of the extracellular space ionic composition and volume is well documented (for review see [19,32,33]). It has been demonstrated that immature or reactive glial cells are not able to control ionic and volume homeostasis [10,32–34]. Stimulation of the CNS leads to an elevation in extracellular K^+ and pH and to glial swelling, which can result in prolonged changes in neuronal excitability, synaptic transmission and glial function, by altering neuronal and glial membrane potentials and transmitter release. The possible role of glia in behaviour and plasticity is supported by many recent studies (for review see [11]). Processes such as glycogenolysis and glutamine synthesis, which in the normal brain occur exclusively in astrocytes, have been shown to play a crucial role in CNS consolidation of memory [8,20,21]. Glial cells are involved in the synthesis and uptake of neurotransmitters and can respond to many of the same communication factors as do neurones [11]. A correlation between astrocytic shape and the number of synapses has been demonstrated by Meshul et al. [16]. These authors suggested that astrocytic ensheathment of synapses provokes a reduction in the number of synapses, thus demonstrating the importance of astrocytes for memory. Structural plasticity accompanied by an increase in glia has been found in rats maintained in an enriched environment and during synaptogenesis related to kindling and the induction of LTP in the hippocampus [11].

This study compares the effect of early postnatal hypobaric hypoxia [7] on behaviour and the histology of the cortex and hippocampus. We tested the spatial memory of rats 3 weeks and 3 months old over a 10-day period in a Morris water maze and studied neuronal density, immunostaining for neurofilaments, astrocytes, and oligodendrocytes, and changes in their morphology.

2. Methods

2.1. Postnatal hypobaric hypoxia

Newborn Wistar rats, together with their mothers, were exposed to a simulated altitude of 7000 m (pO_2 64.4 mmHg) for 8 h per day from birth until the age of 19 days (P19), excluding Days 6, 7, 13 and 14 [7]. The temperature ($24 \pm 1^\circ C$) and humidity ($60 \pm 4\%$) of the air were stable. The altitude was raised at a rate of 333 m/s. The animals were allowed food and water ad libitum and were exposed to hypoxia in their breeding cages. Control animals born on the same day and their mothers were not exposed to hypoxia. All infant rats were weaned at the age of P22. Mortality of the rat pups during the period of exposure to hypoxia did not exceed 5%.

2.2. Spatial memory testing in the Morris water maze

Sixteen hypoxic and 15 control male rat pups were included in the experiments. The animals were kept in plastic cages on natural light cycles, with free access to food and water. The body weight of hypoxic and control animals was measured every day prior to the water maze trial.

The Morris water maze was a circular tank, 0.5 m deep and 0.9 or 2 m in diameter, used to test animals from P23 to P32 and from P100 to P109, respectively. The temperature of the water was maintained at $21^\circ C$. The maze was located in a laboratory room where the arrangement of furniture and other orientation points remained unchanged during the entire experiment. The circular escape platform was made of transparent material with a diameter of 12 cm. The platform was situated in the northeast quadrant of the maze and was submerged 1 cm below the water level. Throughout the experiment the position of the platform remained constant.

An eight-trial training session was performed with each animal on 10 successive days at the ages of P23–P32 and P100–P109. The rat was placed into the maze close to the wall of the tank, facing the wall. The starting location was changed randomly (east, north, west or south quadrant). The time needed to find the platform was recorded. The animal was allowed to remain on the platform after finding it for about 20 s and thus to orient to the visual clues and surroundings of the maze. If the animal failed to find the platform within 60 s, placing the animal on the platform ended the trial.

2.3. Histological studies

Six hypoxic and six control animals at P24, three hypoxic and three control animals at P114, and three hypoxic and three control animals at P240 were used for histological studies. There were no significant differences in any of the measured values between the hypoxic groups at P114 and at P240; the results were therefore pooled together to form one group, P114–P240. Rats were sacrificed by

pentobarbital (200 mg/kg body weight intraperitoneally) and perfused transcardially with phosphate buffer (PB) followed by 4% buffered paraformaldehyde. Frozen, coronal sections (40 μm) were cut and stained by cresyl violet (Nissl staining) or processed for immunohistochemistry using monoclonal antibodies against neurofilaments (anti-NF 160; Boehringer-Mannheim, Germany), astrocytes (anti-GFAP; Boehringer-Mannheim, Germany) and oligodendrocytes (RIP antibody; Developmental Studies Hybridoma Bank, Iowa City, IA).

Twenty-four brain sections from the coronal plane according to the Paxinos and Watson co-ordinates [22] -3.00 to -4.00 mm from bregma were stained from each animal: six with Nissl staining, six with anti-NF 160 antibody, six with anti-GFAP antibody, and six with RIP antibody. Anti-NF 160 and anti-GFAP were diluted to 0.4 mg/ml in PB saline (PBS) containing 1% bovine serum albumin (BSA, Sigma Chemical Co., St. Louis, MO) and 0.2% Triton X-100. The partially purified RIP supernatant was diluted

1:50 in PBS with BSA and 0.2% Triton X-100 added. After overnight incubation in the primary antibodies at 4 °C, the floating sections were washed and processed by using biotinylated anti-mouse secondary antibodies and the peroxidase labelled avidin–biotin complex method (Vectastain Elite, Vector Laboratories, Burlingame, CA). Immune complexes were visualised using 0.05% 3,3'-diaminobenzidine tetrahydrochloride (Sigma) in PBS and 0.02% H_2O_2 .

2.4. Image analysis

Coronal sections of the brain, stained for cresyl violet, GFAP, NF 160, and RIP, were analysed using the image analysis system KS 400 (Carl Zeiss, Jena, Germany).

At P24, P114, and P240, the number of neuronal bodies per 0.01 mm^2 was counted from Nissl-stained sections in square or rectangular fields of the brain (Fig. 1A). The square measured fields (Fig. 1A) were in layer II of the motor cortex (MCII), the somatosensory cortex (SCII), and the primary

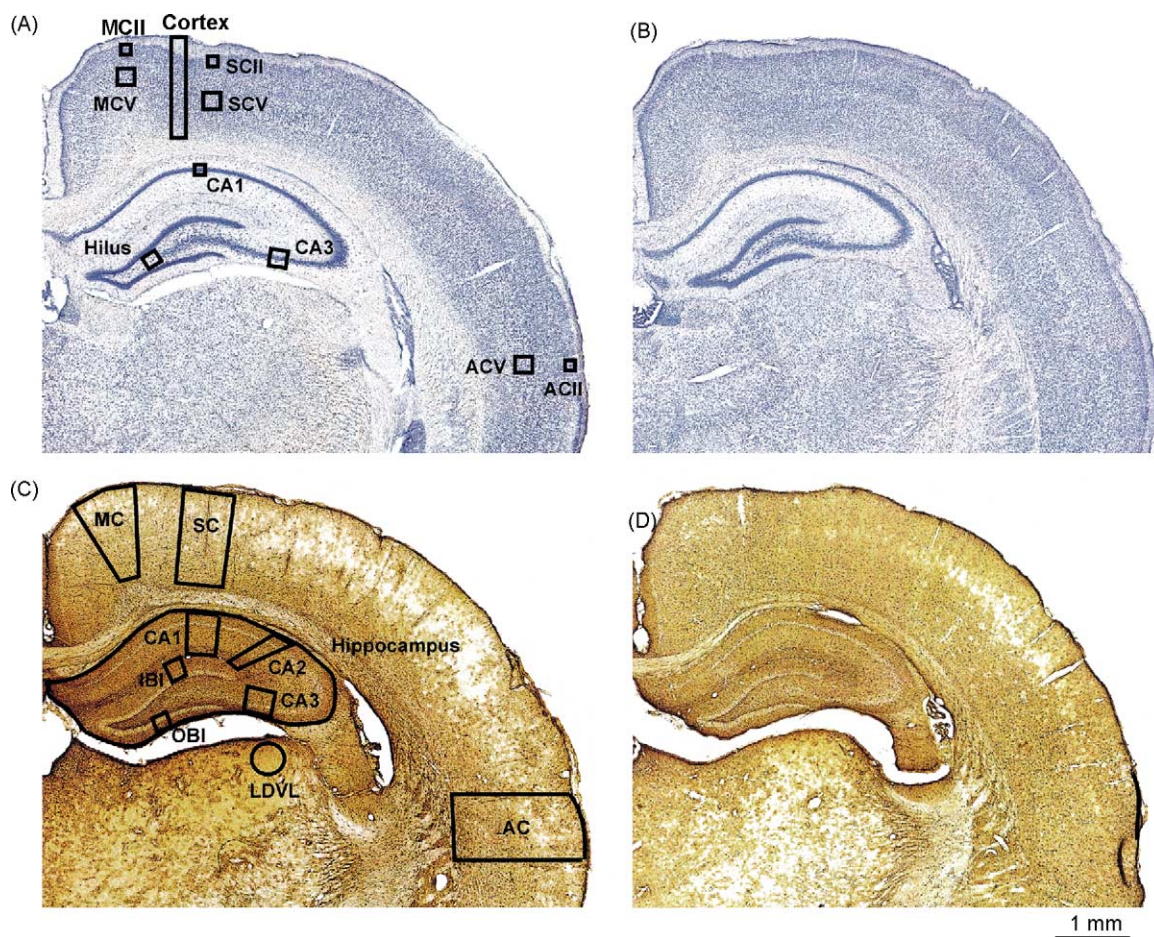


Fig. 1. Coronal sections of 24-day-old rat brains of a normoxic animal and an animal exposed to hypobaric hypoxia showing the areas used for counting neuronal bodies and determining immunostaining optical densities (OD). (A) Control brain, cresyl violet staining; the number of neuronal bodies was measured in these fields: Cortex, MCII, SCII, ACII, MCV, SCV, ACV, CA1, CA3 and Hilus. (B) Brain after hypoxia, cresyl violet staining. (C) GFAP staining; OD were measured in these regions of interest (OD_{ROI}): MC, SC, AC, CA1, CA2, CA3, IB1, OB1 and the whole hippocampus. OD were also measured in a reference region (OD_{REF}) in the ventrolateral part of the thalamic laterodorsal nucleus (LDVL). (D) Brain after hypoxia, GFAP staining. An explanation of the abbreviations and further details of the measurements are given in the text.

auditory cortex (ACII), all fields 0.004 mm²; layer V of the motor cortex (MCV), the somatosensory cortex (SCV), and the primary auditory cortex (ACV), all fields 0.017 mm²; the pyramidal layer of the hippocampal CA1 area (CA1, field: 0.004 mm²); the pyramidal layer of the hippocampal CA3 area (CA3, field: 0.017 mm²) and in the hilus of the dentate gyrus (Hilus, field: 0.025 mm²). The rectangular field measured through the whole cortical thickness (Cortex) was 0.06 mm² in area (Fig. 1A). Neurones were discriminated from other cell types by visual observation of size and shape. Neurones had large oval cell bodies; the small cell bodies of glia or cell body fragments were excluded. Two sections were analysed for each brain.

The optical densities (OD) of immunostaining for NF 160, GFAP and RIP were measured in regions of interest (ROI) in the cortex and hippocampus and in a reference region (REF) with low immunoreactivity in the ventrolateral part of the thalamic laterodorsal nucleus (LDVL, Fig. 1C) at P24, P114, and P240. Relative optical densities (ROD) were calculated as: $ROD = [(OD_{ROI}/OD_{REF}) - 1] \times 100$ [27]. Two sections were analysed for each brain. OD_{ROI} were measured in the primary and secondary motor cortex (MC), the primary somatosensory cortex (SC), and the auditory cortex (AC); measured fields were 0.8–1.2 mm². OD_{ROI} in the hippocampus were measured in an area of 4.5 mm² and then in the separate hippocampal regions CA1 (measured field: 0.3 mm²), CA2 (field: 0.2 mm²), CA3 (field: 0.1 mm²), and the inner (IB1) and outer (OB1) blades of the dentate gyrus (field: 0.1 mm²).

2.5. Statistical analysis

Statistical analysis of the differences between control and hypoxic animals in body weight, neuronal density, OD, and ROD was performed using a one-way analysis of variance (ANOVA) test ($P \leq 0.05$ was considered statistically significant). The mean escape latencies in the Morris water maze of control and hypoxic animals on successive days of testing from P23 to P32 and P100 to P109 were analysed by a two-way ANOVA (groups \times days) with repeated measures on days, followed by the post-hoc Newman–Keuls test [17]; $P \leq 0.05$ was considered statistically significant.

3. Results

3.1. Animal behaviour and body weight

During decompression the mothers were hyperactive and hyperventilating. During exposure to a simulated altitude of 7000 m, they displayed a marked reduction in motor activity and did not provide any care for their pups, who mostly remained in the nest. During recompression following hypoxia, the mothers were again hyperactive and hyperventilating, and their motor activity was increased.

Table 1

Body weight in grams at postnatal Days P23–P32 and P100 of control animals (control) and animals exposed to hypoxia (hypoxic)

Age (days)	Control (n = 15)	Hypoxic (n = 16)
P23	53.33 \pm 1.72	32.50 \pm 0.95*
P24	57.06 \pm 1.99	35.06 \pm 0.90*
P25	60.00 \pm 2.65	38.25 \pm 0.92*
P26	66.40 \pm 2.43	43.37 \pm 0.96*
P27	73.06 \pm 2.17	50.12 \pm 1.79*
P28	76.46 \pm 3.05	53.87 \pm 1.55*
P29	86.00 \pm 2.42	57.25 \pm 1.35*
P30	86.53 \pm 3.29	62.12 \pm 1.87*
P31	92.13 \pm 5.00	64.12 \pm 1.41*
P32	106.00 \pm 2.88	74.87 \pm 2.12*
P100	316.00 \pm 23.45 (n = 14)	311.70 \pm 9.02 (n = 15)

Body weight was measured every day before the trials in the Morris water maze. Data are given as mean \pm S.E.M.

* Significant difference from control ($P < 0.0001$).

After returning to normal conditions, the mothers' care was enhanced; they excreted, and they fed their pups. The pups' behaviour before, during and after hypoxia was related to the age of the animals; animals older than 10 days were more active than younger animals. Motor activity, food intake and maternal care were reduced during hypoxia. Pups exhibited hyperactivity and hyperventilation during decompression and recompression. The pups' behaviour when returned to normoxic conditions did not reveal differences from the control group.

There was a significant decrease ($P < 0.0001$) in the body weight of hypoxic pups at the beginning of the behavioural testing (P23), showing that due to intermittent hypobaric hypoxia, the growth of the animals was retarded (Table 1). The weight gain in the hypoxic group between P23 and P32 was 130% versus 98% for the control group. Body weight at the age of P100 did not differ between hypoxic and control groups.

3.2. Morris water maze

Sixteen hypoxic and 15 control animals were tested for 10 successive days in the Morris water maze from P23 to P32. Place navigation learning in naive rats was slower in hypoxic animals than in controls. The hypoxic rats were significantly slower in finding the platform on Days 2–5 (P23–P26), but reached the same asymptotic level on Days 6–10 (P27–P32, Fig. 2). A two-way ANOVA (groups \times days) with repeated measures on days yielded significant main effects of groups ($F(1, 29) = 5.534$, $P < 0.05$) and of days ($F(9, 261) = 65.3$, $P < 0.001$) as well as a significant interaction ($F(9, 261) = 3.3$, $P > 0.01$). The Newman–Keuls post-hoc test revealed a significant difference in the mean latencies between hypoxic and control groups on the first 8 days. On the other hand, hypoxic rats also showed a progressive reduction in the latency needed to reach the platform. From P28 to P32 the difference between the hypoxic and control groups was not significant.

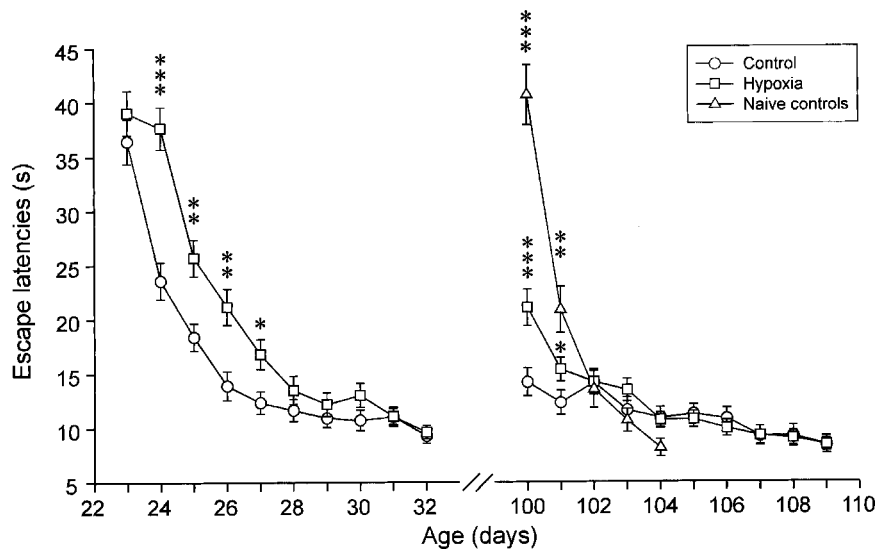


Fig. 2. Mean escape latencies (mean \pm S.E.M.) in the Morris water maze in control animals and animals exposed to hypoxia. Rats were trained from P23 to P32 and from P100 to P109; another group of naive rats was first tested at P100 and trained from P100 to P104. Asterisks indicate significant differences between control and hypoxic animals at the timepoints indicated (*, $P < 0.05$; **, $P < 0.01$; ***, $P < 0.001$).

Fifteen hypoxic and 14 control animals from the young group were tested again for 10 days from P100 to P109. Hypoxic rats had significantly longer escape latencies on Days P100 and P101. Naive Wistar rats tested at the age of P100 had significantly longer escape latencies on the first 2 days of training compared to both control and hypoxic animals previously trained from P23 to P32, who apparently remembered their early postnatal training. A comparison of over-trained place navigation retrieval in hypoxic and control animals and naive rats of the same age showed significant mean effects of groups ($F(2, 33) = 10.87$, $P = 0.0002$) and of days ($F(4, 132) = 44.7$, $P < 0.0001$) as well as a significant interaction ($F(8, 132) = 12.09$, $P < 0.0001$). The Newman–Keuls post-hoc test revealed a significant difference in the mean latencies between naive animals and both control and hypoxic groups on the first 2 days, but not on the remaining Days P102–P104 (Fig. 2).

3.3. Histological changes

At P24, Nissl staining showed that following hypobaric hypoxia, the typical laminar organisation of the motor, somatosensory, and auditory cortical areas was impaired (Fig. 3A–D). In hypoxic rats, more nuclei were found in the cortical grey matter compared to controls in layer II of the motor, somatosensory and primary auditory areas and layer V in the motor area (Table 2). Layer II was thinner with densely packed neurones (Fig. 3A–D). However, when we measured the total number of neuronal cell nuclei throughout the whole cortical thickness, no significant difference was found: the density of neuronal bodies per 0.01 mm^2 was 6.56 ± 0.27 ($n = 6$) in control brains and 6.82 ± 0.25 ($n = 6$) in brains after hypoxia. This suggests

affected cortical morphogenesis and histogenesis and a different distribution of neurones after hypoxia. The cell nuclei densities in the measured hippocampal areas were not significantly different from controls (Table 2).

Relative optical densities were calculated (see Section 2) from the OD of immunostaining for neurofilaments (NF 160), astrocytes (GFAP) and oligodendrocytes (RIP) in control and hypoxic rats. The OD for NF 160, GFAP, and RIP immunostaining in ROI were measured in the cortical and hippocampal areas shown in Fig. 1C. Before calculating the ROD, the optical density of a reference region (OD_{REF}) in the ventrolateral part of the LDVL was measured (Fig. 1C). There were no statistically significant differences in OD_{REF} between control and hypoxic rats.

In hypoxic rats at P24, the relative optical density of the staining for NF 160 was decreased in the motor and somatosensory cortex, in the hippocampus as a whole, in the CA1 region and in the inner blade of the gyrus dentatus compared to controls of the same age (Table 2, Fig. 3E and F). In hypoxic rats, the typical parallel structure of the neuronal processes passing through the granular cell layer was lost (Fig. 4A and B). The whole hippocampal area as observed on coronal sections was significantly smaller in hypoxic rats ($4.24 \pm 0.07 \text{ mm}^2$) compared to control rats ($4.86 \pm 0.08 \text{ mm}^2$).

There were no significant differences between control and hypoxic rats in the relative optical densities of GFAP staining in any area of the cortex (Fig. 3G and H, Table 2). However, astrocytes in hypoxic rats at P24 often showed thicker and shorter processes widespread throughout the cortex, with enlarged end-feet, typical of isomorphic gliosis [2]. Decreased staining for GFAP was found in the hippocampus of hypoxic rats in all measured regions except CA2

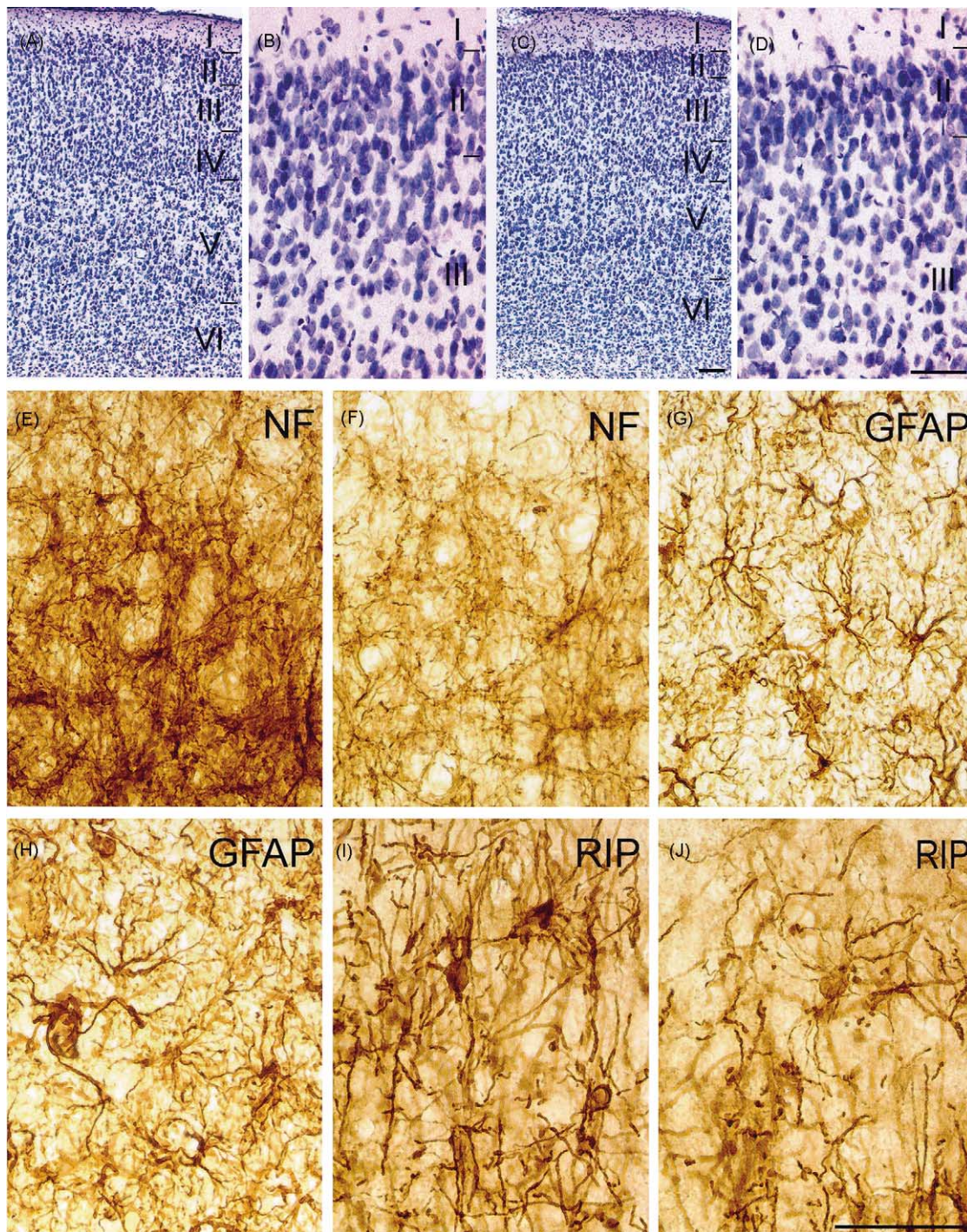


Fig. 3. Changes in neuronal and macroglial structure in the motor cortex in rats at P24 evoked by intermittent hypobaric hypoxia. (A–D) Cresyl violet staining in the primary motor cortex at two different magnifications. (A, B) Control animal, (C, D) animal after hypoxia. Note the decreased thickness of layer II containing densely packed neurones. Lines mark the borders between cortical layers. (E) Dense staining for neurofilaments (NF 160) seen in layers II and III of the primary motor cortex in a control animal; (F) decreased staining for NF 160 in layers II and III of the primary motor cortex after hypoxia; (G) staining for astrocytes (GFAP) in layers II and III of the primary motor cortex in a control animal shows star-shaped astrocytes with fine processes; (H) layers II and III of the primary motor cortex stained for astrocytes in an animal exposed to hypoxia show hypertrophy of distinct processes without a significant increase in the intensity of the staining; (I) staining for oligodendrocytes (RIP) in layers II and III of the primary motor cortex in a control animal shows densely stained cell bodies and processes; (J) layers II and III of the primary motor cortex stained for oligodendrocytes after hypoxia show a decreased staining density and weakly stained processes with an impaired structure. Scale bar shown for A and C in C represents 100 μm , for B and D in D represents 50 μm , and for E–J in J represents 50 μm .

Table 2

Density of neuronal bodies per 10,000 μm^2 in different brain areas at P24 and at P114–P240 in control animals (control) and in animals subjected to intermittent hypobaric hypoxia (hypoxia)

Age (days)	Neuronal density			Relative optical density						
	Area	Control (<i>n</i> = 12)	Hypoxia (<i>n</i> = 12)	Area	NF 160		GFAP		RIP	
					Control (<i>n</i> = 12)	Hypoxia (<i>n</i> = 12)	Control (<i>n</i> = 12)	Hypoxia (<i>n</i> = 12)	Control (<i>n</i> = 12)	Hypoxia (<i>n</i> = 12)
P24	MCII	43.76 ± 3.06	52.51 ± 1.76*	MC	16.96 ± 1.23	11.91 ± 2.12*	25.05 ± 1.42	24.59 ± 1.34	13.01 ± 1.63	6.48 ± 2.25*
	SCII	49.93 ± 1.36	57.09 ± 2.65*	SC	10.70 ± 1.09	4.36 ± 2.79*	25.39 ± 1.44	24.91 ± 0.92	12.50 ± 1.47	3.42 ± 2.35*
	ACII	27.05 ± 1.67	32.02 ± 1.67*	AC	11.89 ± 1.75	10.10 ± 3.18	24.38 ± 0.71	25.41 ± 1.74	6.48 ± 1.10	7.19 ± 2.06
	MCV	11.14 ± 0.67	13.87 ± 0.92*	Hip	7.03 ± 0.82	1.95 ± 1.96*	21.33 ± 0.91	16.71 ± 0.87*	8.71 ± 1.40	5.21 ± 0.84*
	SCV	17.90 ± 0.99	17.40 ± 0.56	CA1	5.93 ± 0.92	0.13 ± 2.53*	19.62 ± 1.04	14.73 ± 1.03*	6.08 ± 0.54	3.12 ± 0.93*
	ACV	13.33 ± 0.72	12.93 ± 0.55	CA2	10.14 ± 1.53	5.72 ± 2.55	22.11 ± 1.17	19.60 ± 0.97	10.32 ± 1.09	8.44 ± 0.82
	CA1	48.14 ± 1.78	48.93 ± 1.75	CA3	8.11 ± 1.44	4.45 ± 2.07	21.71 ± 1.23	16.64 ± 1.25*	6.99 ± 0.88	4.86 ± 1.02
	CA3	17.80 ± 0.84	18.46 ± 0.77	IB1	4.31 ± 0.78	1.70 ± 2.27*	18.51 ± 1.01	12.61 ± 0.93*	5.77 ± 0.53	2.12 ± 0.91*
	Hilus	5.27 ± 0.32	4.77 ± 0.29	OB1	2.31 ± 0.74	0.97 ± 1.52	20.95 ± 1.07	14.40 ± 0.71*	2.22 ± 0.42	3.59 ± 1.30
P114–P240	MCII	51.72 ± 2.22	54.70 ± 1.12	MC	15.68 ± 1.91	18.44 ± 1.52	2.84 ± 3.72	0.38 ± 2.55	7.99 ± 3.56	15.33 ± 1.94
	SCII	52.91 ± 2.13	55.70 ± 2.06	SC	13.99 ± 2.66	12.23 ± 2.53	1.34 ± 3.80	1.88 ± 3.06	1.66 ± 3.84	6.66 ± 3.72
	ACII	49.53 ± 2.04	48.14 ± 1.60	AC	11.33 ± 2.18	11.23 ± 1.81	8.82 ± 3.35	10.83 ± 2.40	0.44 ± 2.27	1.62 ± 2.08
	MCV	16.41 ± 1.39	17.35 ± 0.88	Hip	11.88 ± 2.01	9.56 ± 2.04	1.28 ± 4.33	1.07 ± 0.86	3.94 ± 2.66	0.58 ± 2.19
	SCV	25.36 ± 0.81	23.62 ± 1.12	CA1	11.28 ± 2.19	6.92 ± 2.57	2.26 ± 4.56	0.82 ± 1.63	7.02 ± 2.74	3.05 ± 2.25
	ACV	14.32 ± 0.41	13.92 ± 0.47	CA2	14.91 ± 2.02	14.18 ± 2.21	0.72 ± 4.41	2.32 ± 1.71	2.15 ± 1.87	6.02 ± 1.92
	CA1	50.33 ± 1.67	47.34 ± 1.76	CA3	19.65 ± 1.16	14.96 ± 2.32	0.78 ± 4.70	3.03 ± 1.09	0.13 ± 2.19	5.57 ± 2.14
	CA3	18.65 ± 0.84	17.95 ± 0.50	IB1	8.71 ± 2.06	3.95 ± 2.43	5.54 ± 4.40	3.09 ± 1.32	7.42 ± 2.68	5.42 ± 2.54
	Hilus	5.34 ± 0.30	5.54 ± 0.37	OB1	13.47 ± 1.30	10.55 ± 2.80	0.87 ± 4.65	1.79 ± 1.72	0.85 ± 3.20	0.71 ± 2.56

Relative optical densities in control and hypoxic animals at P24 and at P114–P240 of immunostaining for neurofilaments (NF 160), astrocytes (GFAP) and oligodendrocytes (RIP).

The density of neuronal bodies was measured in layer II of the motor cortex (MCII), the somatosensory cortex (SCII) and the primary auditory cortex (ACII); in layer V of the motor cortex (MCV), the somatosensory cortex (SCV) and the primary auditory cortex (ACV); the hippocampal regions CA1 and CA3; and the hilus of the dentate gyrus (Hilus). See Fig. 1A for a schematic drawing of the measured fields. The optical densities (OD) of immunostaining for NF 160, GFAP and RIP were measured in regions of interest (ROI): the primary and secondary motor cortex (MC), the primary somatosensory cortex (SC) and the primary auditory cortex (AC); the hippocampus as a whole (Hip); the hippocampal regions CA1, CA2 and CA3; the inner (IB1) and outer (OB1) blades of the dentate gyrus; and in a reference region in the ventrolateral part of the thalamic laterodorsal nucleus (LDVL). See Fig. 1C for a schematic drawing of the measured fields. At P24, the mean OD_{REF} for NF 160 was 167.89 ± 4.88 in control brain and 164.04 ± 5.68 after hypoxia; the mean OD_{REF} for GFAP was 241.94 ± 3.22 in control brain and 237.55 ± 2.84 after hypoxia; and the mean OD_{REF} for RIP was 213.69 ± 1.26 in control brain and 214.08 ± 2.12 after hypoxia. At P114–P240 the mean OD_{REF} for NF 160 was 213.19 ± 2.97 in control brain and 206.97 ± 3.08 after hypoxia; the mean OD_{REF} for GFAP was 173.96 ± 5.45 in control brain and 166.79 ± 4.45 after hypoxia; and the mean OD_{REF} for RIP was 213.19 ± 2.97 in control brain and 206.97 ± 3.08 after hypoxia. Relative optical densities (ROD) were calculated as: $\text{ROD} = [(\text{OD}_{\text{ROI}}/\text{OD}_{\text{REF}}) - 1] \times 100$. Results of the measurements are expressed as the mean \pm S.E.M.; details about the measurements are given in the text.

* Significant difference from control ($P < 0.05$).

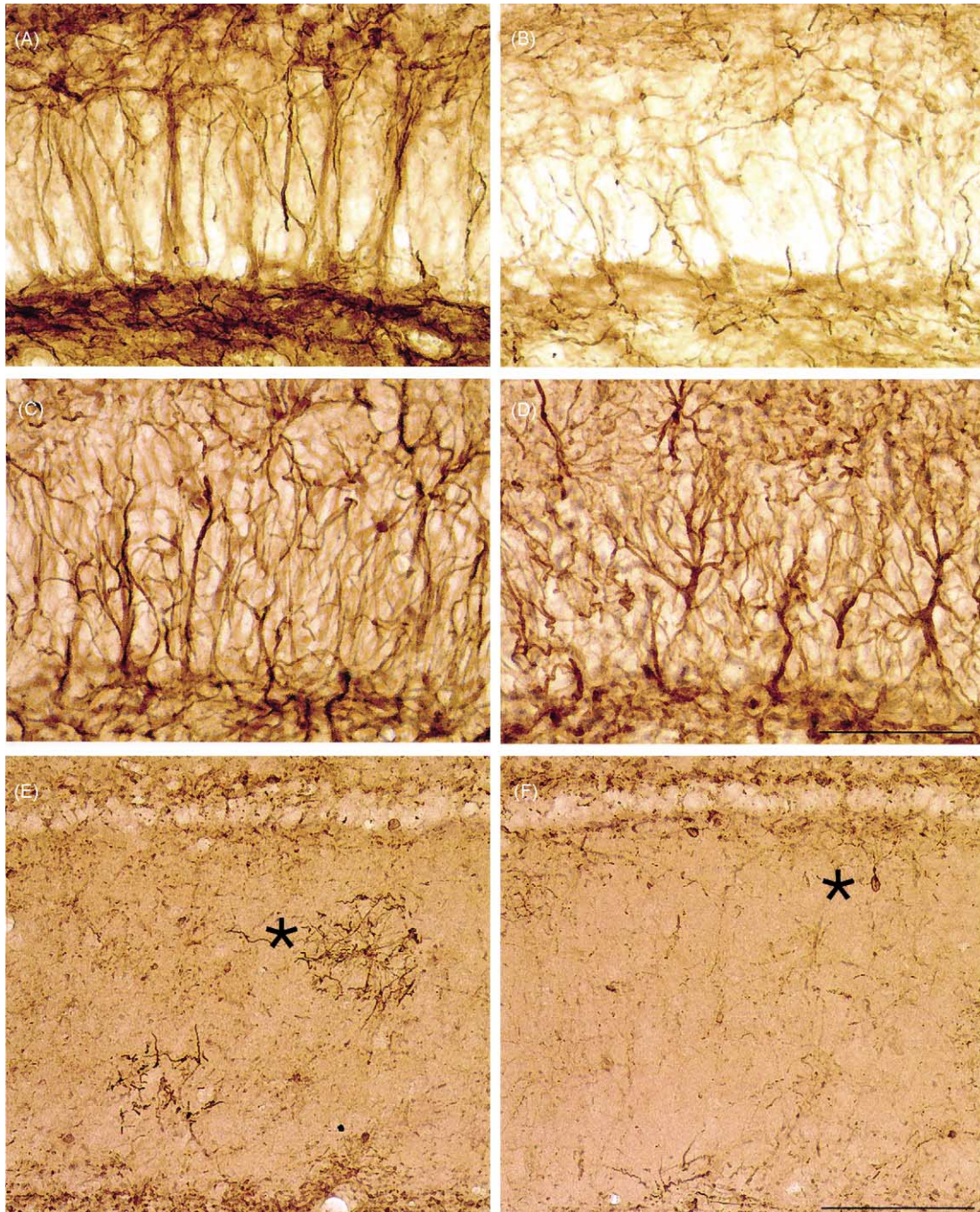


Fig. 4. Changes in neuronal and macroglial structure in the hippocampus evoked by intermittent hypobaric hypoxia. (A) The granular layer of the inner blade of the dentate gyrus stained for NF 160 in a control animal at P24 shows the parallel organisation of the neurofilaments passing through the neuronal layer. (B) Staining for NF 160 in the granular layer at P24 in an animal exposed to hypoxia shows decreased staining and a loss of the parallel organisation of the neuronal processes. (C) The granular layer of the inner blade of the dentate gyrus stained for astrocytes in a control animal at P114 shows parallel glial processes passing through the neuronal layer. (D) Staining for astrocytes in the granular layer in an animal exposed to hypoxia shows decreased staining and a loss of the parallel organisation of the glial processes. (E) The CA1 layer of the hippocampus stained for oligodendrocytes in a control animal at P240 shows the parallel organisation of glial processes passing through the pyramidal layer and numerous processes radiating from an oligodendrocytic cell body in the stratum radiatum (asterisk). (F) Staining for oligodendrocytes in the CA1 layer after hypoxia at P240 shows a decreased number of glial processes radiating from a cell body in the stratum radiatum (asterisk). Scale bar shown for A–D in D represents 50 μm ; scale bar shown for E and F in F represents 100 μm .

(Table 2). The astrocytic processes passing through the granular cell layer lacked the parallel organisation characteristic of the control animals [35,36].

At P24 the relative optical density of RIP staining for oligodendrocytes decreased in hypoxic rats as compared to controls in the motor cortex, the somatosensory cortex, the hippocampus as a whole, CA1 and IB1, but not in the auditory cortex, CA2, CA3, or OB1 (Table 2). In hypoxic brains, RIP-positive oligodendrocytes had fewer processes than in control rats, especially in cortical layers II–IV. The parallel organisation of the processes in the hippocampus was diminished (Fig. 3I and J).

At P114 and P240, there was no difference in the cell body densities of animals subjected to hypoxia and controls (Table 2); the thickness of the hippocampus decreased in hypoxic animals, but the size of the total hippocampal area was not significantly different between the two groups: $4.94 \pm 0.23 \text{ mm}^2$ in controls and $4.63 \pm 0.13 \text{ mm}^2$ after hypoxia. The density of the staining for NF 160 in the cortex of hypoxic rats was not significantly different from that seen in control rats (Table 2). GFAP staining in the cortex and hippocampus of hypoxic animals revealed a hypertrophy of astrocytic processes and also an impaired parallel organisation of the astrocytic processes, particularly in the granular layer of the dentate gyrus (Fig. 4C and D). No difference in ROD was observed compared to controls of the same age (Table 2). Moreover, we found a decreased number of oligodendrocytic processes in both the cortex and hippocampus of hypoxic animals at P114–P240 as compared to controls of the same age (Fig. 4E and F), but there was no significantly decreased ROD in hypoxic animals compared to controls (Table 2).

4. Discussion

Testing spatial memory in the Morris water maze is a generally accepted method for detecting spatial memory deficits in both young and adult rats [18]. All rats are equally motivated to escape from water; there is no need for food or water deprivation; swimming is an inborn ability of rat pups; and the problem of scent is eliminated in comparison with a dry maze. In our study we used Wistar rats. When evaluating the cognitive memory and memory deficits of Wistar rats, it must be taken into account that albino rats are less efficient in orienting in the Morris water maze than are pigmented rats. Albinism is connected with several visual defects, both anatomical and functional [1], and orientation in the Morris water maze is primarily a visual task.

Intermittent hypobaric hypoxia is widely used as an animal model of perinatal neuronal hypoxic insult [7,12,37]. Trojan et al. [37] observed decreased body weight up to the 33rd day, similarly as in our experiment; and young experimental animals displayed greater motor activity under conditions of hypoxia. The development of unconditioned reflexes was not impaired; the young hypobaric animals

elaborated a conditioned defense reflex better than controls but differential inhibition worse than controls [37].

The spatial memory of adult rats after hypobaric hypoxia has been reported to be impaired [31]. Dell'Anna et al. [4] observed transient hyperactivity and spatial memory deficits in 20- to 45-day-old rats that were exposed to 25 min of anoxia induced by 100% N₂ exposure at 30 h after birth. They detected impaired spatial memory in a maze between P30 and P40 using food as a reward and in a water maze between P50 and P60. Longo and Hermans [14] found no difference in escape latencies in a Morris water maze between rats exposed to prenatal hypoxia (10.5% O₂ 4 h per day) and control rats on P29. This is in agreement with our findings that the ability to locate a platform on the first day of training is the same in hypoxic animals as in controls (Fig. 2). However, in our study we did further training, which revealed statistically significant differences showing that hypoxic animals learn the task much slower than do the controls. If training continues for 6 or more days, hypoxic rats finally perform as well as the controls. Similar observations were made in humans by Zubrick et al. [39]. Children with perinatal hypoxic–ischemic injury attained similar levels of performance as did their healthy classmates in academic tests of reading, spelling or arithmetic, but it took them longer to reach any given level of performance. A comparison between adult control and hypoxic rats and adult naive rats shows that both control and hypoxic animals trained when young remember the task until adulthood, and they only have to learn the position of the platform again. However, adult hypoxic rats again learn the task significantly more slowly than do the controls, but faster than when they were young and untrained.

At P24, we observed in hypoxic animals increased neuronal cell density in layers II and V of the motor cortex and in layer II of the somatosensory and auditory cortex, but the density of neurones in the hippocampus was not different from controls of the same age (Table 2). Furthermore, the density of neurones measured throughout the whole cortical thickness was not changed. The density of neuronal bodies in control brains was higher in every measured field in adult brains at P114–P240 than at P24 (Table 2). Hypoxic injury during the postnatal period accelerated migration into these layers, but the final number of neuronal bodies in adulthood was the same in controls as in hypoxic animals. Shukitt-Hale et al. [30] have shown that in adult rats during exposure to simulated altitudes of 5950 and 6400 m, the number of damaged neurones is significantly increased in the CA3 region of the hippocampus.

The changes in the structure of glial processes observed in our study as a consequence of hypoxia-induced brain damage have not been described previously. Based on our results, we suggest that immature astrocytes and oligodendrocytes in newborn rats are more sensitive to anoxia than are mature glial cells and that hypoxia can delay their maturation. Indeed, we found smaller oligodendrocytes with fewer processes in hypoxic rats (Fig. 3I and J; Fig. 4E

and F). The decreased ROD of oligodendrocytic staining found in our study in both the cortex and hippocampus of hypoxic animals at P24 correlates well with previously published results of delayed myelination in the corpus callosum, which was observed by electron microscopy after intermittent hypobaric hypoxia [12].

The abnormal organisation of astrocytic processes—thicker end-feet in the cortex and a loss of parallel organisation in the hippocampus—observed in our study suggests that hypobaric hypoxia impairs gliogenesis similarly as do degenerative changes during aging [35,36], which in young animals can lead to atypical neuronal migration and maturation. It was shown previously that hypoxia also affects dendritic arborisation in the cortex and hippocampus [7,23], which correlates with the lack of fine astrocytic processes and the disorganisation of astrocytic process structure observed in our study (Fig. 3G and H; Fig. 4C and D). Changes in astrocyte morphology have been shown to impair anisotropic diffusion in the hippocampus of aged rats with learning deficits in a water maze [36]. In the present study, the fine changes in glial organisation persisting in adult rats at P114–P240 suggest that these animals might be more prone to learning deficits, e.g. under pathological conditions or during aging.

The observed changes in the organisation of astrocytic and oligodendrocytic processes in our study resemble those found in aging rats with impaired learning [36], but there is one difference. In this study we observed weaker staining for the astrocytic marker and structural protein GFAP, which suggests that the changes are different from classical injury-evoked gliosis. Dell' Anna et al. [5] found enhanced GFAP staining at P7 in the hippocampus of rats that were exposed to 25 min of anoxia induced by 100% N₂ exposure at 30 h after birth, while no differences between anoxic and control animals were observed at later time-points. Rodnight et al. [24] showed that in the hippocampus, the mechanism of GFAP phosphorylation is different in slices from young rats (P12–P16) than in slices from adult rats. In adults the phosphorylation is dependent only on the extracellular concentration of [Ca²⁺], but in young animals it is dependent on both glutamate and [Ca²⁺]. Elevated glutamate together with high external Ca²⁺ levels, as well as a lack of both glutamate and external Ca²⁺, enhance GFAP phosphorylation, which regulates the dynamic equilibrium between the polymerised and depolymerised states of GFAP filaments and plays a fundamental role in mitosis. The authors suggested that glutamate liberated from developing synapses during the period of synaptogenesis at P12–P16 may signal an increase in the number of mitotic astrocytes [24]. We can therefore speculate that a sustained lack of glutamate release during the period of hypoxic exposure, when the animals were inactive, could decrease astrocyte proliferation and could lead to the observed down-regulation of GFAP staining in the hippocampus after hypoxia.

Intermittent hypobaric hypoxia from birth until the age of 19 days evoked substantial changes in fine glial morphology

that persisted until adulthood. These structural changes could lead to the impaired spatial learning observed after hypoxic exposure in young as well as adult animals.

Acknowledgements

The authors thank Dr. Dana Marešová for providing hypoxic rats. This work was supported by grants from the Czech Ministry of Education, Sports and Youth J13/98 111300004 and LN00S065, and from the Academy of Sciences of the Czech Republic AVOZ5039906.

References

- [1] Andrews JS. Possible confounding influence of strain, age and gender on cognitive performance in rats. *Brain Res Cogn Brain Res* 1996;3:251–67.
- [2] Bignami A, Dahl B. Gliosis. In: Kettenmann H, Ransom BR, editors. *Neuroglia*. New York: Oxford University Press; 1995. p. 843–58.
- [3] Brichová H. Ultrastructural image of the cerebral cortex of rats exposed to hypobaric altitude hypoxia. I. The neuroglia and tissue capillaries of young animals after early termination of hypoxia. *Folia Morphol* 1984;32:384–90.
- [4] Dell' Anna ME, Calzolari S, Molinari M, Iuvone L, Calimici R. Neonatal anoxia induces transitory hyperactivity, permanent spatial memory deficits and CA1 cell density reduction in developing rats. *Behav Brain Res* 1991;45:125–34.
- [5] Dell' Anna ME, Geloso MC, Draisci G. Transient changes in Fos and GFAP immunoreactivity precede neuronal loss in the rat hippocampus following neonatal anoxia. *Exp Neurol* 1995;131:144–56.
- [6] Fenton AA, Bures J. Place navigation in rats with unilateral TTX inactivation of the dorsal hippocampus: place but not procedural learning can be lateralised to one hippocampus. *Behav Neurosci* 1993;107:552–64.
- [7] Fisher J, Jílek L, Trojan S. Quantitative and qualitative neurohistological changes produced in the rat brain by prolonged aerogenic hypoxia in early ontogeny. *Physiol Bohemosl* 1974;23:211–9.
- [8] Gibbs ME, O'Dowd BS, Hertz L, Robinson SR, Sedman GR, Ng KT. Inhibition of glutamine synthetase activity prevents memory consolidation. *Cog Brain Res* 1996;4:57–64.
- [9] Grafe MR. Developmental changes in the sensitivity of the neonatal rat brain to hypoxic/ischemic injury. *Brain Res* 1994;653:161–6.
- [10] Jendelová P, Syková E. Role of glia in K⁺ and pH-homeostasis in the neonatal rat spinal cord. *Glia* 1991;4:56–63.
- [11] Laming PR, Kimelberg H, Robinson S, Salm A, Hawrylak N, Müller C, et al. Ng K neuronal–glial interactions and behaviour. *Neurosci Biobehav Rev* 2000;24:295–340.
- [12] Langmeier M, Pokorný J, Mareš J, Trojan S. Changes of the neuronal structure produced by prolonged hypobaric hypoxia in infant rats. *Biomed Biochem Acta* 1989;48:S204–207.
- [13] Langmeier M, Pokorný J, Mareš J, Mareš P, Trojan S. Effects of prolonged hypobaric hypoxia during postnatal development on myelination of corpus callosum in rats. *J Hinforsch* 1987;4:385–95.
- [14] Longo LD, Hermans HM. Behavioural and neurochemical sequelae in young rats of antenatal hypoxia. *Early Hum Dev* 1992;29:83–90.
- [15] Lun A, Dominic B, Gross J. An animal model of perinatal hypoxic brain damage: behavioural aspects. *Biomed Biochim Acta* 1990;49:1021–6.
- [16] Meshul CK, Seil FJ, Herndon RM. Astrocytes play a role in regulation of synaptic density. *Brain Res* 1987;402:139–45.

- [17] Moghaddam M, Bures J. Rotation of water in the Morris water maze interferes with path integration mechanisms of place navigation. *Neurobiol Learn Mem* 1997;68:239–51.
- [18] Morris RGM. Spatial localization does not require the presence of local cues. *Learn Motiv* 1981;12:239–60.
- [19] Nicholson C, Syková E. Extracellular space structure revealed by diffusion analysis. *Trends Neurosci* 1998;21:207–15.
- [20] O'Dowd BS, Gibbs ME, Ng KT, Hertz E, Hertz L. Astrocytic glykogenolysis energizes intermediate memory processes in neonate chicks. *Dev Brain Res* 1994;78:137–41.
- [21] O'Dowd BS, Gibbs ME, Sedman G, Ng KT. Astrocytes implicated in the energizing of intermediate memory processes in neonate chicks. *Cogn Brain Res* 1994;2:93–102.
- [22] Paxinos G, Watson C. The rat brain in stereotaxic coordinates. San Diego, CA: Academic Press; 1997.
- [23] Pokorný J, Trojan S, Fisher J. Changes of the rat hippocampus after prolonged postnatal hypoxia. *Physiol Bohemosl* 1982;31:193–202.
- [24] Rodnight R, Goncalves CA, Wofchuk ST, Leal R. Control of the phosphorylation of the astrocyte marker glial fibrillary acidic protein (GFAP) in the immature rat hippocampus by glutamate and calcium ions: positive key factor in astrocytic plasticity. *Braz J Med Biol Res* 1997;30:325–38.
- [25] Rudy JW, Stadler-Morris S, Albert P. Ontogeny of spatial navigation behaviors in the rat: dissociation of “proximal”- and “distal”-cue-based behaviors. *Behav Neurosci* 1987;101:62–73.
- [26] Sadowski M, Wisniewski HM, Jakubowska-Sadowska K, Tarnawski M, Lazarewicz JW, Mossakowski MJ. Pattern of neuronal loss in the rat hippocampus following experimental cardiac arrest-induced ischemia. *J Neurol Sci* 1999;168:13–20.
- [27] Scheffler B, Faissner A, Beck H, Behle K, Wolf HK, Wiestler OD, et al. Hippocampal loss of tenascin boundaries in Ammon's horn sclerosis. *Glia* 1997;19:35–46.
- [28] Schenk F. Development of place navigation in rats from weaning to puberty. *Behav Neural Biol* 1985;43:69–85.
- [29] Schmidt-Kastner B, Freund TF. Selective vulnerability of the hippocampus in brain ischemia. *Neuroscience* 1991;40:599–636.
- [30] Shukitt-Hale B, Kadar T, Marlowe BE, Stillman MJ, Galli RL, Levy A, et al. Morphological alterations in the hippocampus following hypobaric hypoxia. *Hum Exp Toxicol* 1996;15:312–9.
- [31] Shukitt-Hale B, Stillman MJ, Welch DI, Levy A, Devine JA, Lieberman HR. Hypobaric hypoxia impairs spatial memory in an elevation-dependent fashion. *Behav Neurol Biol* 1994;62:244–52.
- [32] Syková E. Ionic and volume changes in the microenvironment of nerve and receptor cells. In: Autrum H, Ottoson D, Perl ER, Schmidt RF, Shimazu H, Willis WD, editors. *Progress in sensory physiology*. New York: Springer; 1992. p. 167.
- [33] Syková E. The extracellular space in the CNS: its regulation, volume and geometry in normal and pathological neuronal function. *Neuroscientist* 1997;3:28–41.
- [34] Syková E, Jendelová P, Svoboda J, Sedman G, Ng KT. Activity-related rise in extracellular potassium concentration in the brain of 1–3-day-old chicks. *Brain Res Bull* 1990;24:569–75.
- [35] Syková E, Mazel T, Šimonová Z. Diffusion constraints and neuron–glia interaction during aging. *Exp Gerontol* 1998;33: 837–51.
- [36] Syková E, Mazel T, Hasenöhrl RU, Harvey AR, Šimonová Z, Mulders WHAM, et al. Learning deficits in aged rats related to decrease in extracellular volume and loss of diffusion anisotropy in hippocampus. *Hippocampus* 2002;12:469–79.
- [37] Trojan S, Jílek L, Staudacherová D, Trávníčková E. Adaptation of rats to repeated aerogenic hypoxia in early postnatal ontogenesis and adulthood. *Physiol Bohemosl* 1974;23:199–209.
- [38] Zimmer C, Sampaolo S, Shanker Sharma H, Cervós-Navarro J. Altered glial fibrillary acidic protein immunoreactivity in rat brain following chronic hypoxia. *Neuroscience* 1991;40:353–61.
- [39] Zubrick SR, Macartney H, Stanley FJ. Hidden handicap in school-age children who received neonatal intensive care. *Dev Med Child Neurol* 1988;30:145–52.